Ionics (2018) 24:1111–1119
DOI 10.1007/s11581-017-2257-9

ORIGINAL PAPER

Palladium nanoparticles supported on phosphorus-doped carbon for ethanol electro-oxidation in alkaline media

Júlio César M. Silva[1] · **Isabel C. de Freitas**[1] · **Almir O. Neto**[1] · **Estevam V. Spinacé**[1] · **Vilmaria A. Ribeiro**[1]

Received: 12 April 2017 / Revised: 31 July 2017 / Accepted: 16 August 2017 / Published online: 2 September 2017

Abstract Palladium nanoparticles supported on carbon Vulcan XC72 (Pd/C) and on phosphorus-doped carbon (Pd/P-C) were prepared by an alcohol reduction process. X-ray diffractograms of Pd/C and Pd/P-C showed the typical face-centered cubic (fcc) structure of Pd. The crystallite sizes of Pd fcc phase were around 8 nm for both samples. X-ray photoelectron spectroscopy revealed to Pd/C and Pd/P-C that Pd was found predominantly in the metallic state and to Pd/P-C, the presence of P increases the amount of oxygen on the electrocatalyst surface. The activity and stability of the electrocatalyts for ethanol electro-oxidation in alkaline medium was investigated by cyclic voltammetry and chronoamperometry experiments. The peak current density on Pd/P-C was 50% higher than on Pd/C, while the current density measured after 30 min at − 0.35 V vs. Hg/HgO was 65% higher on Pd/P-C than on Pd/C. The enhancement of the catalytic activity of Pd/P-C electrocatalyst might be related to the presence of higher amounts of oxygen species on the surface, which could contribute to the oxidation of intermediates formed during ethanol electro-oxidation process.

Keywords Palladium nanoparticles · Phosphorus-doped carbon · Ethanol electro-oxidation · Alkaline media

Introduction

The search for new energy sources, which is based on the concept of clean and renewable energy, has been intensified in the recent years [1–3]. In this context, fuel cells may offer an excellent alternative to the current energy generation as a clean and efficient power source [4–7]. Polymer electrolyte membrane fuel cells (PEMFCs) represent a promising alternative for transport and stationary power generation [8–10]. Thus, this technology could significantly contribute to the reduction of greenhouse gas emissions [11]. Different fuels have been proposed to feed these devices, e.g., methanol [4, 12], ethylene glycol [6, 13], formic acid [14, 15], and ethanol [5, 8].

Among the different possible fuels, ethanol is considered promising due to its high energy density (8.0 kW kg^{-1}), low toxicity, and for being a renewable fuel obtained from the biomass [16–19]. The complete oxidation of ethanol to CO_2 produces 12 electrons per ethanol molecule [5, 19–21]. However, to oxidize ethanol to CO_2, the C–C bond splitting is required, which is difficult in low temperatures [5, 19, 20]. As a consequence, acetaldehyde and acetic acid (acetate in alkaline media), which produce 2 and 4 electrons per ethanol molecule, respectively, are the main products [19, 22], which represent considerable loss in the faradic efficiency to the process [23, 24]. Although the production of CO_2 from ethanol electro-oxidation is difficult, it occurs [25], and CO is an intermediate to the CO_2 formation, which adsorbs on the catalyst surface, blocking the activity sites for ethanol electro-oxidation, acting as a poisoning species [26].

It has been reported that the ethanol electro-oxidation kinetic in alkaline media is enhanced compared to the acid media [7, 27]. According to the literature, palladium shows higher catalytic activity than platinum for ethanol electro-oxidation in alkaline media [26, 28–33]. This aspect is very important because palladium is more abundant and less expensive than platinum [28, 34, 35]. However, the catalytic activity of palladium towards ethanol electro-oxidation can be improved by introducing a second or a third element, producing

✉ Vilmaria A. Ribeiro
vilmariaap@gmail.com

[1] Instituto de Pesquisas Energéticas e Nucleares, IPEN/CNEN-SP, Av. Prof. Lineu Prestes, 2242 Cidade Universitária, CEP, São Paulo, SP 05508-900, Brazil

bimetallic or multimetallic palladium-based electrocatalysts, such as PdAu/C, PdAg/C, and PdCuPb/C [30, 31, 36, 37]. The synergic effect of Pd with different metals was also observed for different oxidation reactions, such as ethylene glycol [38, 39], glycerol [13, 40], and glucose [41].

The electrocatalysts are usually synthesized as nanoparticles and anchored on a support material, which is usually carbon black due to its large surface area, high electrical conductivity, porous structures, and low cost [42, 43]. However, this support material does not enhance the catalytic activity of the electrocatalysts, but serves mostly as a mechanical support [44–47]. In order to improve the catalytic activity of the materials, carbon has been doped with different elements, such as P, N, B, S, and Se [48, 49]. Among these elements, phosphorus is an interesting choice since it has 5 electrons in its outer electronic orbit which might alter the electron distribution of the metal nanoparticles [50]. It is also reported that the presence of phosphorus into the carbon support materials increase the amount of oxygen on the electrocatalysts, which is beneficial to oxidize poisoning species, like CO, for example [51, 52].

Song et al. [51] investigated the influence of phosphorus as dopant into ordered mesoporous carbon used as support for platinum nanoparticles for methanol and CO electro-oxidation. It was seen that the presence of phosphorus increased the amount of oxygen on the material and shifted the onset of CO and methanol electro-oxidation to lower overpotential compared to the same catalyst without phosphorus.

According to Li et al. [50], the oxidation peak of CO electro-oxidation was negatively shifted on Pd/P-C compared to Pd/C, which was attributed to the higher amount of oxygen groups on Pd/P-C. The electrocatalytic activity of Pd/P-C for formic acid oxidation was also higher than Pd/C [50].

In the present study, palladium nanoparticles were supported on carbon and phosphorus-doped carbon. The materials were used as electrocatalysts for ethanol electro-oxidation in alkaline media. The objective was to investigate the beneficial effect of phosphorus-doping carbon into the electrocatalysts as already shown for electro-oxidation of methanol, formic acid, and CO [50, 51].

Experimental

Phosphorus-doped carbon was prepared based on the method presented in reference [53]. In this process, certain amount of phosphoric acid (corresponding 3% in mass ratio of the carbon) was inserted to the Vulcan XC72 Cabot (previously treated at in a tubular oven at 800 °C under argon atmosphere) and heated (10 °C min^{-1}) under argon atmosphere in a tubular furnace at 800 °C for 1 h.

Palladium nanoparticles supported on carbon and phosphorus-doped carbon (20 wt% of metal loading) were synthesized by a modified alcohol reduction process related previously [54], using $Pd(NO_3)_2{\cdot}2H_2O$ (Sigma-Aldrich) as the metallic precursor. In this process, $Pd(NO_3)_2{\cdot}2H_2O$ was diluted in a solution containing three parts of ethylene glycol and one of water (*v*/*v*), then appropriated amount of carbon or phosphorus-doped carbon was subsequently added. The dispersion was kept in an ultrasonic bath for 20 min and then submitted to reflux for 3 h under open atmosphere at 150 °C. The resulting electrocatalysts were filtered, washed with deionized water, and dried in an oven at 70 °C for 2 h.

A Rigaku diffractometer model Miniflex II using Cu Kα radiation source (0.15406 nm) was used to perform the X-ray diffraction (XRD) analysis. The X-ray diffraction patterns were recorded with a step size of 0.05° and a scan time of 2 s per step from 2θ = 20° to 90°. A JEOL transmission electron microscope (TEM) model JEM-2100 operated at 200 kV was used to obtain information about the sizes and distribution of the nanoparticles. The size distribution and mean particle sizes were performed by measuring about 200 nanoparticles from different regions of the electrocatalysts.

The X-ray photoelectron spectroscopy (XPS) analyses were done with an SPECSLAB II (Phoibos-Hsa 3500 150, 9 channeltrons) SPECS spectrometer, with Al Kα source (E = 1486.6 eV) working at 15 kV, Epass = 40 eV, 0.2 eV energy step, and 2 s per point was the acquisition time. The synthesized electrocatalysts were kept on stainless steel sample holders and transported under inert atmosphere to the prechamber of the XPS staying there in a vacuum atmosphere for 2 h. The residual pressure inside the analysis chamber was ~ 1×10^{-9} Torr. The binding energies (BE) of the Pd 3d, P 2p, O 1s, and C 1s spectral peaks were referenced to C 1s peak, at 284.5 eV, providing accuracy within ± 0.2 eV.

Electrochemical measurements were performed with a potentiostat/galvanostat PGSTAT 302N Autolab at room temperature in a three-electrode cell made of Teflon. As reference electrode and counter electrode, a Hg/HgO and a platinum foil were used. A glassy carbon (GC) with the geometric area of 0.031 cm^2 was the working electrodes to support the synthesized electrocatalysts. Alumina (1 μm) was employed to polish the GC support before each experiment. In all experimental procedures, ultrapure water obtained from a Milli-Q system (Millipore®) was used.

The working electrodes were constructed by dispersing 6 mg of the electrocatalyst powder in 900 μL of water, 100 μL of isopropyl alcohol, and 40 μL of 5% Nafion®. Then, the mixture was dispersed in an ultrasonic bath for 30 min. Shortly thereafter, aliquots of 10 μL of the dispersion fluid were deposited onto the GC surface and dried for 20 min at 60 °C.

Cyclic voltammograms (CV) in ethanol-free solutions were carried out at the potential range of − 0.85 to 0.1 V vs. Hg/HgO at a scan rate of 20 mV s^{-1}. The electrocatalysts were cycled for five consecutive cycles in the 1 mol L^{-1} KOH solution, resulting in the reproducible shape of the CVs. The

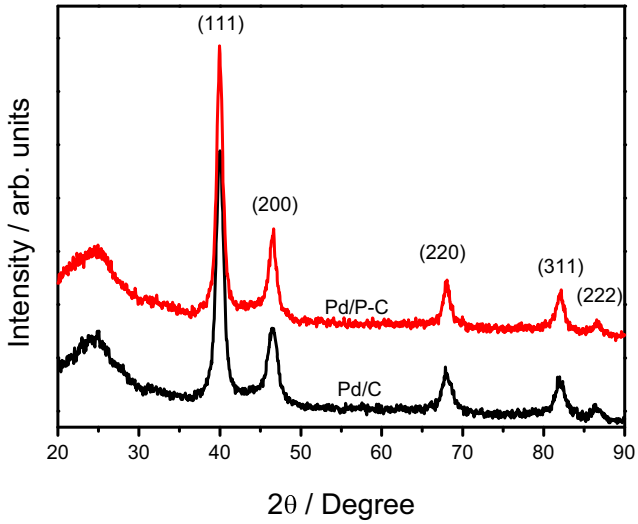

Fig. 1 X-ray diffraction patterns of Pd/C and Pd/P-C electrocatalysts

ethanol electro-oxidation was investigated by the CV experiments in the presence of 1 mol L^{-1} ethanol in 1 mol L^{-1} KOH, carried out at a scan rate of 20 mV s^{-1} between − 0.85 and 0.1 V vs. Hg/HgO. The electrocatalysts were cycled for three consecutive cycles and the third cycle is shown. Chronoamperometric experiments were carried out at − 0.35 V vs. Hg/HgO for 30 min.

The catalyst electrochemical active surface area (ECSA) was determined by stripping experiments of CO monolayers, integrating the CO_{ad} stripping charges, assuming the factor of 420 μC cm^{-2} [55]. The experiment was performed in 1 mol L^{-1} KOH, carried out at a scan rate of 20 mV s^{-1} between − 0.85 and 0.1 V vs. Hg/HgO. The working electrode was polarized at − 0.6 V and carbon monoxide was bubbled during 20 min into electrolyte, followed by nitrogen gas for 20 min [56]. The estimated ECSA values for Pd/C and Pd/P-C were 34.1 m^2 per grams of Pd.

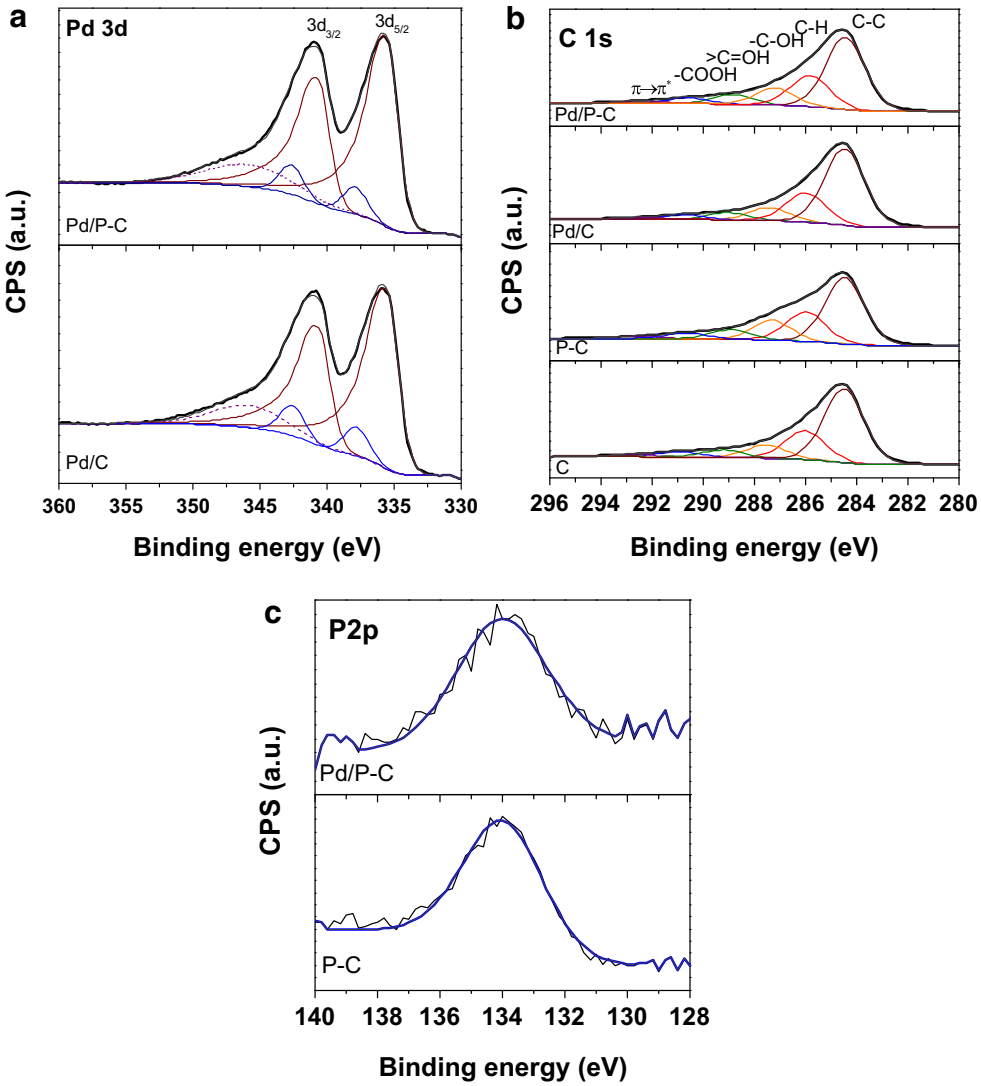

Fig. 2 Fitted XPS Pd 3d (**a**), C 1s (**b**), and P 2p (**c**) of C, P-C, Pd/C, and Pd/P-C samples

Table 1 XPS characteristics of Pd $4f_{5/2}$, P 2p, and O 1s regions for C, P-V, Pd/C, and Pd/P-C samples

Samples	Binding energy (eV)					
	Pd $3d_{5/2}$		P 2p	O 1s		
	Pd^0	Pd^{2+}		O_L	O_S	O_C O_W
C	n.d.	n.d.	n.d.	528.9 (8)	531.2 (83)	534.4 (9)
P-C	n.d.	n.d.	133.9	529.4 (12)	531.6 (79)	534.4 (9)
Pd/C	335.6 (91)	337.9 (9)	n.d.	529.6 (33)	531.5 (55)	534.6 (12)
Pd/P-C	335.6 (92)	337.8 (8)	134.0	529.8 (32)	531.5 (58)	534.7 (10)

Percent of species

n.d. not determined

Results and discussion

The X-ray diffractograms of Pd/C and Pd/P-C electrocatalysts are shown in Fig. 1. In all XRD patterns, a broad peak at about $2\theta = 25°$ due to the (022) reflection of the hexagonal structure of Vulcan XC 72 carbon was observed [57, 58]. Peaks corresponding to the palladium face-centered cubic (fcc) structure can be seen at approximately $2\theta = 39°$, 46°, 67°, and 81° that correspond to (111), (200), (220), and (311) planes, respectively [16, 59]. Using the Scherrer equation and (220) peak, the mean crystallite size of the materials was estimated [17, 60]. The obtained values were 9.2 and 8.1 nm for Pd/P-C and Pd/C, respectively.

In order to investigate the surface composition and the oxidation state of the elements present in the eletrocatalyst XPS, analyses were performed for the samples and the results are presented in Fig. 2 and Tables 1 and 2. As shown in Fig. 2a, Pd 3d region exhibits a doublet (i.e., $3d_{5\backslash2}$ and $3d_{3\backslash2}$) with a spin-orbit splitting of about ~ 5.2 eV, in agreement with the literature [61–63]. In this study, the Pd $3d_{5/2}$ peak gives two contributions at 335.6 and 337.9 eV, which on the basis of their binding energies can be assigned to two different states of palladium, Pd^0 and Pd^{2+}, respectively [61, 63, 64]. As it can be seen in Table 1, the surfaces of Pd/C and Pd/P-C are predominantly in the metallic state, 91 and 92%, respectively. The feature at 346.3 eV is most likely a plasmon loss band associated with the peak at 335.6 eV [64, 65].

The C 1s spectrum (Fig. 2b) was deconvoluted into six peaks [66]. The peak at about 284.4 eV is assigned to graphitic carbon phase, whereas the peak related to hydrocarbons (C–H) from defects in the graphitic structure is around 286 eV [66–68]. Additionally, peaks corresponding to carbon–oxygen bonding structures (–C–OH, >C=O, and –COOH), and a peak assigned to $\pi \rightarrow \pi*$ plasmon excitation values [66, 68], can be seen in Table 1. The O 1s peak (Table 1) consists of three components at about 529, 531, and 534 eV, which are attributed to the lattice oxygen (O_L), surface oxygen species bonded to carbon support or metal atoms (O_S), and oxygen atoms bonded to carbon by double bonds (O_C) and/or adsorbed water (O_W), respectively [66]. From Tables 1 and 2, it is possible to see that the P-C and Pd/P-C have higher percentage of oxygen on the surface than C and Pd/C; consequently, it is possible to conclude that the presence of phosphorus into the carbon support increases the amount of oxygen on the electrocatalyst surface, which is in agreement with the literature [50, 51].

In Fig. 2c, it is possible to observe the peak related to P 2p at around 134 eV [51, 59]. Although it is possible to observe a peak related to phosphorus element, the presence of phosphorus on the surface is only in very small amount. However, it is clear that the phosphorus is present into the carbon.

Figure 3 shows the TEM micrographs and histogram of the palladium particle sizes. The palladium nanoparticles supported on carbon (Fig. 3a) and phosphorus-doped carbon (Fig. 3b)

Table 2 XPS characteristics of C 1s region for C, P-C, Pd/C, and Pd/P-C samples

Sample	Binding energy C 1s (eV)						Peak intensity (%)
	Peak I C–C	Peak II C–H (defects)	Peak III –C–OH	Peak IV >C=O	Peak V –COOH	Peak VI $\pi \rightarrow \pi^*$	I_{Oxy}/I_C**[b]
C	284.5 (56)*[a]	286.0 (22)	287.5 (10)	289.2 (6)	290.9 (4)	292.8 (2)	19
P-CP	284.5 (50)	286.0 (22)	287.3 (15)	288.9 (6)	290.7 (5)	292.5 (2)	26
Pd/C	284.5 (57)	286.0 (22)	287.4 (10)	289.0 (5)	290.7 (4)	292.5 (2)	19
Pd/P-C	284.5 (52)	285.9 (23)	287.2 (12)	288.9 (7)	290.6 (4)	292.5 (2)	24

[a] Percent of species

[b] Intensity of three oxygen-containing functional groups (peaks III–V) in % of total C 1s area

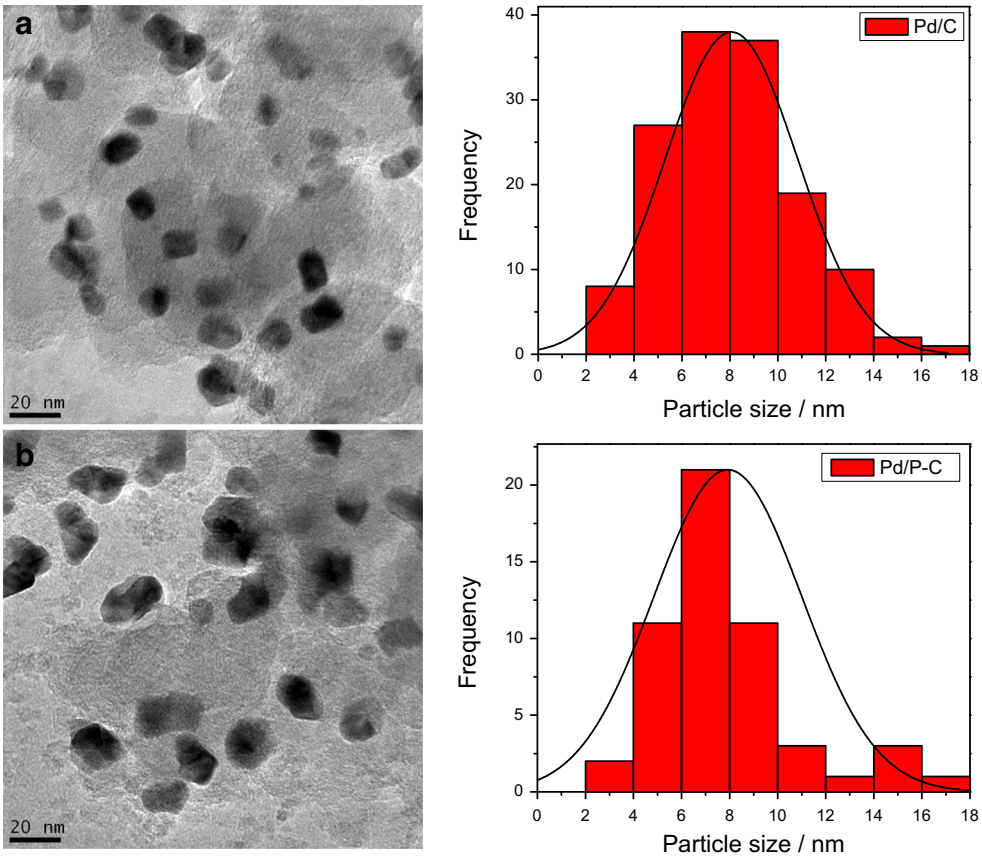

Fig. 3 TEM micrographs of Pd/C (**a**) and Pd/P-C (**b**) electrocatalysts, and the respective histograms

are relatively well dispersed on the material support. In the corresponding histograms, it is possible to see that the nanoparticle sizes are from 2 to 18 nm, but the highest percentage of them are smaller than 10 nm. The particle mean size of Pd/C is 7.92 ± 3.08 nm and Pd/P-C is 8.06 ± 2.76 nm, which are in good concordance with the mean crystallite size estimated by Scherrer equation and are in agreement with the nanoparticle sizes of the catalysts synthesized by the same method [69, 70].

The cyclic voltammetry of the electrocatalysts in 1 mol L^{-1} KOH in the potential range of − 0.85 to 0.1 V are shown in Fig. 4. As it can be seen, the CV shape of palladium in alkaline media is similar from that reported in the literature [10, 33, 71]. The region from − 0.20 to 0.1 V (forward scan) is related to the palladium oxide formation and in the reverse scan, a peak at about − 0.2 V represents the reduction of palladium oxide [10, 72]. The peak at around − 0.4 V related to OH adsorption on Pd/C [10, 73] is slightly shifted to higher

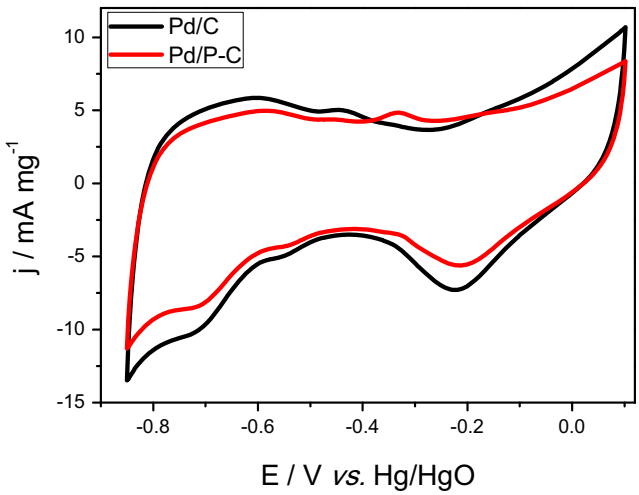

Fig. 4 Voltammograms of Pd/C and Pd/P-C in 1 mol L^{-1} KOH at 20 mV s^{-1}

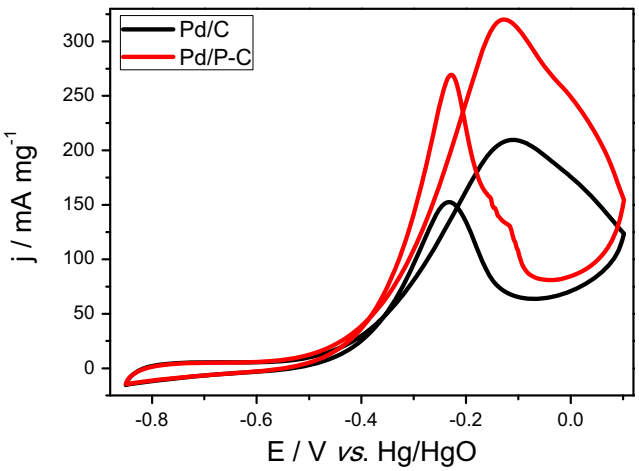

Fig. 5 Voltammograms of Pd/C and Pd/P-C in 1 mol L^{-1} KOH + 1 mol L^{-1} ethanol at 20 mV s^{-1}

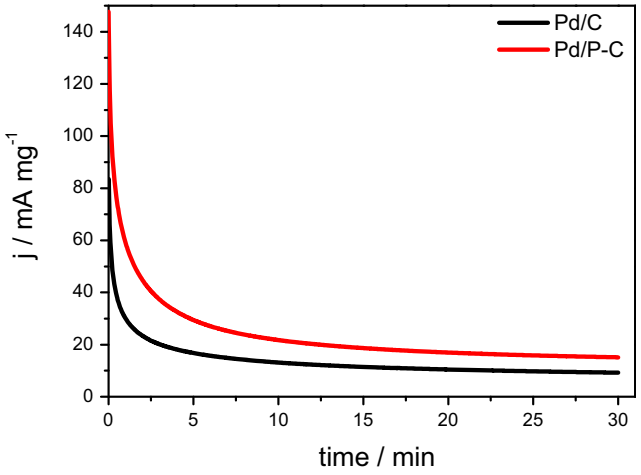

Fig. 6 Chronoamperometric results at − 0.35 V of Pd/C and Pd/P-C in 1 mol L^{-1} KOH + 1 mol L^{-1} ethanol

overpotential on Pd/P-C. As it can be observed, the presence of phosphorus into the carbon support did not lead to significant changes in the shape of the CVs of palladium electrocatalysts as also observed in the literature [50].

Cyclic voltammetry was used to study the electrocatalytic activity of the Pd/C and Pd/P-C towards ethanol electro-oxidation. Figure 5 shows the CVs in 1 mol L^{-1} KOH + 1 mol L^{-1} ethanol. The presence of phosphorus into carbon support enhanced the catalytic activity of palladium electrocatalysts. The peak current density from ethanol electro-oxidation on Pd/P-C was about 50% higher than on Pd/C. Furthermore, the onset potential for ethanol electro-oxidation on Pd/P-C was slightly lower than on the material without phosphorus. The onset potential is related to the thermodynamics of the process; thus, the thermodynamics of ethanol electro-oxidation is favored on Pt/P-C [74, 75]. However, the higher current density obtained on CV experiments is also related to the kinetic of the process [74, 75]. Therefore, the results obtained suggest that the ethanol electro-oxidation on Pt/P-C is favored in terms of thermodynamic and kinetic.

Li et al. [50] supported palladium nanoparticles on phosphorus-doping carbon and observed that the catalytic activity of the palladium nanoparticles towards formic acid electro-oxidation was enhanced if compared to palladium supported on carbon. According to the authors, the presence of phosphorus into carbon support improves the CO removal of palladium nanoparticle surface, which was associated with the higher amount of oxygen groups on the phosphorus-doped carbon electrocatalysts. Song et al. [51] reported that platinum nanoparticles supported on phosphorus-doped ordered mesoporous carbon (Pt/POMC) show higher catalytic activity towards methanol electro-oxidation in the acid medium than platinum supported on ordered mesoporous carbon (Pt/OMC). They attributed the enhancement in the catalytic activity to the higher oxygen content on Pt/POMC electrocatalysts.

It is important to point out that the XPS analysis showed higher percentage of oxygen on the Pd/P-C electrocatalyst than on Pd/C. Thus, the highest catalytic activity of Pd/P-C towards ethanol electro-oxidation might be related to an improvement on the oxidation of adsorbed species on the catalyst surface as seen for methanol and formic acid electro-oxidation [50, 51].

Figure 6 displays the chronoamperometric curves obtained by polarization at − 0.35 V during 30 min in the presence of 1 mol L^{-1} ethanol + 1 mol L^{-1} KOH. As in the CV experiments, a better result was obtained with Pd/P-C than Pd/C electrocatalyst. The presence of higher amount of oxygen on the Pd/P-C might have improved the tolerance to the poisoning species, as discussed earlier [50, 51]. The current density for ethanol electro-oxidation at the end of the experiment using Pd/P-C was ~ 65% higher than on Pd/C. Thus, it is evident the improvement of the catalytic activity of palladium electrocatalyst towards ethanol electro-oxidation caused by the presence of phosphorus as dopant into the carbon support material.

The current densities from ethanol electro-oxidation were also normalized per ECSA. Figure 7a shows the peak current density values of the forward scan, and Fig.7b the current density values obtained in the end of the CA experiments. As it can be seen, for both normalization, Pd/P-C shows higher catalytic activity than Pd/C.

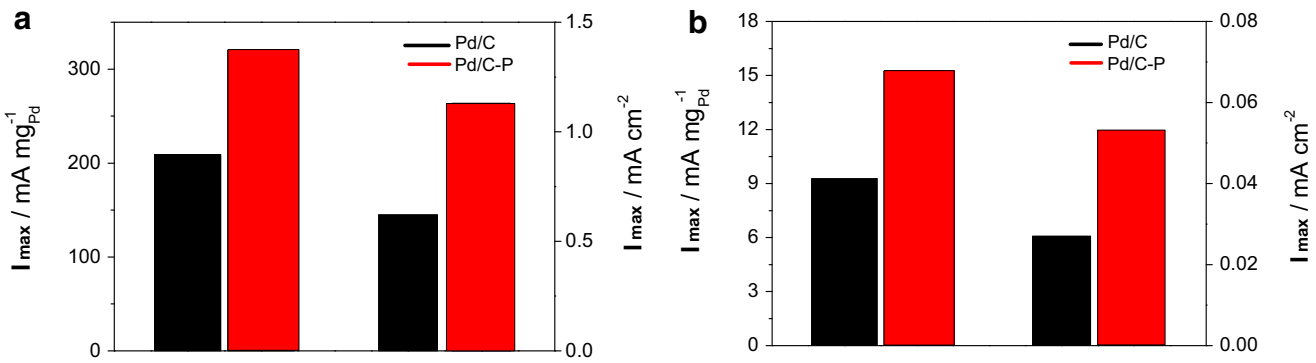

Fig. 7 Peak current density in the CV forward scan (**a**) and the current density obtained in the end of the CA experiments (**b**). Values obtained from ECSA area and per Pd mass

It is important to point out that a lot of papers are focused on preparing binary or multimetallic Pd-based materials supported on carbon. In the present study, it was shown that the catalyst activity of palladium electrocatalysts can be improved by doping the carbon support with phosphorus. Thus, in future works, the synergic effect of the phosphorus-doping carbon support with bimetallic or multimetallic Pd-based materials can be investigated for ethanol electro-oxidation.

Conclusions

In this work, it was shown that the ethanol electro-oxidation on palladium nanoparticles can be improved by doping the carbon support with phosphorus. According to the TEM micrographs, the mean particle sizes were 8.06 ± 2.76 for Pd/P-C and 7.92 ± 3.08 Pd/C. The XPS analysis revealed that the presence of phosphorus into the carbon support increased the amount of oxygen on the catalyst surface which is beneficial to improve the catalytic activity of the palladium electrocatalysts towards ethanol electro-oxidation. In CV experiments, it was seen that the onset potential of ethanol electro-oxidation was slightly shifted to lower overpotential by the presence of phosphorus into carbon support. Furthermore, the peak current density from ethanol electro-oxidation on Pd/P-C was 50% higher than on Pd/C. In the CA analysis, the current density measured at the end of the experiment was 65% higher on Pd/P-C than on Pd/C. The improvement in the catalytic activity might be related to the higher amount of oxygen on the electrocatalyst containing phosphorus, which could contribute to the oxidation of intermediate products formed during ethanol electro-oxidation process.

Acknowledgements The authors wish to thank CNPq (Proc. Nos. 166089/2015-0, 402850/2015-7, 168251/2014-0, and 310051/2012-6), FAPESP (Proc. No. 2014/09087-4), and CAPES for the financial support. We also thank the Brazilian Synchrotron Light Laboratory (LNLS) for the access to the XPS facility, for the use of TEM facilities (JEOL JEM-2100F) of LNNano-CNPEM, and Dr. Daniela Coelho de Oliveira for the XPS analysis support.

References

1. Chen C-Y, Lai W-H, Yan W-M, Chen C-C, Hsu S-W (2013) Effects of nitrogen and carbon monoxide concentrations on performance of proton exchange membrane fuel cells with Pt–Ru anodic catalyst. J Power Sources 243:138–146. https://doi.org/10.1016/j.jpowsour.2013.06.003
2. Nachiappan N, Kalaignan GP, Sasikumar G (2013) Effect of nitrogen and carbon dioxide as fuel impurities on PEM fuel cell performances. Ionics 19(2):351–354. https://doi.org/10.1007/s11581-012-0730-z
3. Jain SL, Lakeman B, Pointon KD, Irvine JTS (2007) Carbon–air fuel cell development to satisfy our energy demands. Ionics 13(6):413–416. https://doi.org/10.1007/s11581-007-0161-4
4. Kim M-S, Fang B, Chaudhari NK, Song M, Bae T-S, Yu J-S (2010) A highly efficient synthesis approach of supported Pt-Ru catalyst for direct methanol fuel cell. Electrochim Acta 55(15):4543–4550. https://doi.org/10.1016/j.electacta.2010.03.007
5. Zignani SC, Baglio V, Linares JJ, Monforte G, Gonzalez ER, Aricò AS (2012) Performance and selectivity of PtxSn/C electro-catalysts for ethanol oxidation prepared by reduction with different formic acid concentrations. Electrochim Acta 70:255–265
6. Qi J, Benipal N, Liang C, Li W (2016) PdAg/CNT catalyzed alcohol oxidation reaction for high-performance anion exchange membrane direct alcohol fuel cell (alcohol = methanol, ethanol, ethylene glycol and glycerol). Appl Catal B Environ 199:494–503. https://doi.org/10.1016/j.apcatb.2016.06.055
7. Santasalo-Aarnio A, Tuomi S, Jalkanen K, Kontturi K, Kallio T (2013) The correlation of electrochemical and fuel cell results for alcohol oxidation in acidic and alkaline media. Electrochim Acta 87:730–738. https://doi.org/10.1016/j.electacta.2012.09.100
8. Antolini E, Gonzalez ER (2010) Alkaline direct alcohol fuel cells. J Power Sources 195(11):3431–3450. https://doi.org/10.1016/j.jpowsour.2009.11.145
9. Zhu LD, Zhao TS, Xu JB, Liang ZX (2009) Preparation and characterization of carbon-supported sub-monolayer palladium decorated gold nanoparticles for the electro-oxidation of ethanol in alkaline media. J Power Sources 187(1):80–84. https://doi.org/10.1016/j.jpowsour.2008.10.089
10. Geraldes AN, da Silva DF, Pino ES, da Silva JCM, de Souza RFB, Hammer P, Spinacé EV, Neto AO, Linardi M, dos Santos MC (2013) Ethanol electro-oxidation in an alkaline medium using Pd/C, Au/C and PdAu/C electrocatalysts prepared by electron beam irradiation. Electrochim Acta 111:455–465. https://doi.org/10.1016/j.electacta.2013.08.021
11. Maffei N, Pelletier L, McFarlan A (2008) A high performance direct ammonia fuel cell using a mixed ionic and electronic conducting anode. J Power Sources 175(1):221–225. https://doi.org/10.1016/j.jpowsour.2007.09.040
12. Tsiouvaras N, Martínez-Huerta MV, Paschos O, Stimming U, Fierro JLG, Peña MA (2010) PtRuMo/C catalysts for direct methanol fuel cells: effect of the pretreatment on the structural characteristics and methanol electrooxidation. Int J Hydrog Energy 35(20):11478–11488. https://doi.org/10.1016/j.ijhydene.2010.06.053
13. Geraldes AN, da Silva DF, e Silva LG, Spinacé EV, Neto AO, dos Santos MC (2015) Binary and ternary palladium based electrocatalysts for alkaline direct glycerol fuel cell. J Power Sources 293:823–830. https://doi.org/10.1016/j.jpowsour.2015.06.010
14. Mikolajczuk-Zychora A, Borodzinski A, Kedzierzawski P, Mierzwa B, Mazurkiewicz-Pawlicka M, Stobinski L, Ciecierska E, Zimoch A, Opałło M (2016) Highly active carbon supported Pd cathode catalysts for direct formic acid fuel cells. Appl Surf Sci 388(Part B):645–652. https://doi.org/10.1016/j.apsusc.2016.02.065
15. Tsujiguchi T, Matsuoka F, Hokari Y, Osaka Y, Kodama A (2016) Overpotential analysis of the direct formic acid fuel cell. Electrochim Acta 197:32–38. https://doi.org/10.1016/j.electacta.2016.03.062
16. Neto AO, da Silva SG, Buzzo GS, de Souza RFB, Assumpção MHMT, Spinacé EV, Silva JCM (2014) Ethanol electrooxidation on PdIr/C electrocatalysts in alkaline media: electrochemical and fuel cell studies. Ionics:1–9. https://doi.org/10.1007/s11581-014-1201-5
17. Silva JCM, Anea B, De Souza RFB, Assumpcao MHMT, Calegaro ML, Neto AO, Santos MC (2013) Ethanol oxidation reaction on

IrPtSn/C Electrocatalysts with low Pt content. J Braz Chem Soc 24(10):1553–1560. https://doi.org/10.5935/0103-5053.20130196
18. Tayal J, Rawat B, Basu S (2011) Bi-metallic and tri-metallic Pt–Sn/C, Pt–Ir/C, Pt–Ir–Sn/C catalysts for electro-oxidation of ethanol in direct ethanol fuel cell. Int J Hydrog Energy 36(22):14884–14897
19. Shen SY, Zhao TS, Xu JB (2010) Carbon supported PtRh catalysts for ethanol oxidation in alkaline direct ethanol fuel cell. Int J Hydrog Energy 35(23):12911–12917
20. Sun C-L, Tang J-S, Brazeau N, Wu J-J, Ntais S, Yin C-W, Chou H-L, Baranova EA (2015) Particle size effects of sulfonated graphene supported Pt nanoparticles on ethanol electrooxidation. Electrochim Acta 162:282–289. https://doi.org/10.1016/j.electacta.2014.12.099
21. Godoi DRM, Perez J, Villullas HM (2009) Effects of alloyed and oxide phases on methanol oxidation of Pt-Ru/C nanocatalysts of the same particle size. J Phys Chem C 113(19):8518–8525. https://doi.org/10.1021/jp8108804
22. Beyhan S, Uosaki K, Feliu JM, Herrero E (2013) Electrochemical and in situ FTIR studies of ethanol adsorption and oxidation on gold single crystal electrodes in alkaline media. J Electroanal Chem 707:89–94. https://doi.org/10.1016/j.jelechem.2013.08.034
23. Sieben JM, Duarte MME (2012) Methanol, ethanol and ethylene glycol electro-oxidation at Pt and Pt–Ru catalysts electrodeposited over oxidized carbon nanotubes. Int J Hydrog Energy 37(13):9941–9947. https://doi.org/10.1016/j.ijhydene.2012.01.173
24. González-Quijano D, Pech-Rodríguez WJ, Escalante-García JI, Vargas-Gutiérrez G, Rodríguez-Varela FJ (2014) Electrocatalysts for ethanol and ethylene glycol oxidation reactions. Part I: effects of the polyol synthesis conditions on the characteristics and catalytic activity of Pt–Sn/C anodes. Int J Hydrog Energy 39(29):16676–16685. https://doi.org/10.1016/j.ijhydene.2014.04.125
25. Neto AO, da Silva SG, Buzzo GS, de Souza RFB, Assumpção MHMT, Spinacé EV, Silva JCM (2015) Ethanol electrooxidation on PdIr/C electrocatalysts in alkaline media: electrochemical and fuel cell studies. Ionics 21(2):487–495. https://doi.org/10.1007/s11581-014-1201-5
26. Chen H, Xing Z, Zhu S, Zhang L, Chang Q, Huang J, Cai W-B, Kang N, Zhong C-J, Shao M (2016) Palladium modified gold nanoparticles as electrocatalysts for ethanol electrooxidation. J Power Sources 321:264–269. https://doi.org/10.1016/j.jpowsour.2016.04.072
27. Cui G, Song S, Shen PK, Kowal A, Bianchini C (2009) First-principles considerations on catalytic activity of Pd toward ethanol oxidation. J Phys Chem C 113(35):15639–15642. https://doi.org/10.1021/jp900924s
28. Zhang F, Zhou D, Zhou M (2016) Ethanol electrooxidation on Pd/C nanoparticles in alkaline media. J Energy Chem 25(1):71–76. https://doi.org/10.1016/j.jechem.2015.10.013
29. Nguyen ST, Ling Tan DS, Lee J-M, Chan SH, Wang JY, Wang X (2011) Tb promoted Pd/C catalysts for the electrooxidation of ethanol in alkaline media. Int J Hydrog Energy 36(16):9645–9652. https://doi.org/10.1016/j.ijhydene.2011.05.049
30. Huang Y, Guo Y, Wang Y, Yao J (2014) Synthesis and performance of a novel PdCuPb/C nanocatalyst for ethanol electrooxidation in alkaline medium. Int J Hydrog Energy 39(9):4274–4281. https://doi.org/10.1016/j.ijhydene.2013.12.176
31. Li G, Jiang L, Jiang Q, Wang S, Sun G (2011) Preparation and characterization of PdxAgy/C electrocatalysts for ethanol electrooxidation reaction in alkaline media. Electrochim Acta 56(22):7703–7711. https://doi.org/10.1016/j.electacta.2011.06.036
32. Cai J, Huang Y, Guo Y (2014) PdTex/C nanocatalysts with high catalytic activity for ethanol electro-oxidation in alkaline medium. Appl Catal B Environ 150–151:230–237. https://doi.org/10.1016/j.apcatb.2013.11.035
33. Peng C, Hu Y, Liu M, Zheng Y (2015) Hollow raspberry-like PdAg alloy nanospheres: high electrocatalytic activity for ethanol oxidation in alkaline media. J Power Sources 278:69–75. https://doi.org/10.1016/j.jpowsour.2014.12.056
34. Wang P, Lin X, Yang B, Jin J-M, Hardacre C, Yu N-F, Sun S-G, Lin W-F (2015) Activity enhancement of tetrahexahedral Pd nanocrystals by bi decoration towards ethanol electrooxidation in alkaline media. Electrochim Acta 162:290–299. https://doi.org/10.1016/j.electacta.2015.02.177
35. Mao H, Wang L, Zhu P, Xu Q, Li Q (2014) Carbon-supported PdSn–SnO2 catalyst for ethanol electro-oxidation in alkaline media. Int J Hydrog Energy 39(31):17583–17588. https://doi.org/10.1016/j.ijhydene.2014.08.079
36. Liu C, Cai X, Wang J, Liu J, Riese A, Chen Z, Sun X, Wang S-D (2016) One-step synthesis of AuPd alloy nanoparticles on graphene as a stable catalyst for ethanol electro-oxidation. Int J Hydrog Energy 41(31):13476–13484. https://doi.org/10.1016/j.ijhydene.2016.05.194
37. Ma L, Chu D, Chen R (2012) Comparison of ethanol electro-oxidation on Pt/C and Pd/C catalysts in alkaline media. Int J Hydrog Energy 37(15):11185–11194. https://doi.org/10.1016/j.ijhydene.2012.04.132
38. Wang W, Yang Y, Liu Y, Wang F, Kang Y, Lei Z (2016) Dealloyed different atom ratios Pdx(FeCo)10–x nanoparticle: promising electrocatalyst towards ethylene glycol oxidation. Int J Hydrog Energy 41(1):300–306. https://doi.org/10.1016/j.ijhydene.2015.10.101
39. Xu H, Yan B, Zhang K, Wang J, Li S, Wang C, Shiraishi Y, Du Y, Yang P (2017) Synthesis and characterization of core-shell PdAu convex nanospheres with enhanced electrocatalytic activity for ethylene glycol oxidation. J Alloys Compd 723:36–42. https://doi.org/10.1016/j.jallcom.2017.06.230
40. Wang W, Kang Y, Yang Y, Liu Y, Chai D, Lei Z (2016) PdSn alloy supported on phenanthroline-functionalized carbon as highly active electrocatalysts for glycerol oxidation. Int J Hydrog Energy 41(2):1272–1280. https://doi.org/10.1016/j.ijhydene.2015.11.017
41. Wang W, Dong Y, Xu L, Dong W, Niu X, Lei Z (2017) Combining bimetallic-alloy with selenium functionalized carbon to enhance electrocatalytic activity towards glucose oxidation. Electrochim Acta 244:16–25. https://doi.org/10.1016/j.electacta.2017.05.078
42. Silva JCM, Piasentin RM, Spinacé EV, Neto AO, Baranova EA (2016) The effect of antimony-tin and indium-tin oxide supports on the catalytic activity of Pt nanoparticles for ammonia electro-oxidation. Mater Chem Phys 180:97–103. https://doi.org/10.1016/j.matchemphys.2016.05.047
43. Antolini E (2016) Nitrogen-doped carbons by sustainable N- and C-containing natural resources as nonprecious catalysts and catalyst supports for low temperature fuel cells. Renew Sust Energ Rev 58:34–51. https://doi.org/10.1016/j.rser.2015.12.330
44. Lee K-S, Park I-S, Cho Y-H, Jung D-S, Jung N, Park H-Y, Sung Y-E (2008) Electrocatalytic activity and stability of Pt supported on Sb-doped SnO2 nanoparticles for direct alcohol fuel cells. J Catal 258(1):143–152
45. Chan K-Y, Ding J, Ren J, Cheng S, Tsang KY (2004) Supported mixed metal nanoparticles as electrocatalysts in low temperature fuel cells. J Mater Chem 14(4):505–516. https://doi.org/10.1039/b314224h
46. Park K-W, Sung Y-E, Han S, Yun Y, Hyeon T (2003) Origin of the enhanced catalytic activity of carbon nanocoil-supported PtRu alloy electrocatalysts. J Phys Chem B 108(3):939–944. https://doi.org/10.1021/jp0368031
47. Park I-S, Park K-W, Choi J-H, Park CR, Sung Y-E (2007) Electrocatalytic enhancement of methanol oxidation by graphite nanofibers with a high loading of PtRu alloy nanoparticles. Carbon 45(1):28–33
48. Daems N, Sheng X, Vankelecom IFJ, Pescarmona PP (2014) Metal-free doped carbon materials as electrocatalysts for the oxygen

reduction reaction. J Mater Chem A 2(12):4085–4110. https://doi.org/10.1039/C3TA14043A
49. Daimon H, Kurobe Y (2006) Size reduction of PtRu catalyst particle deposited on carbon support by addition of non-metallic elements. Catal Today 111(3–4):182–187. https://doi.org/10.1016/j.cattod.2005.10.023
50. Li J, Tian Q, Jiang S, Zhang Y, Wu Y (2016) Electrocatalytic performances of phosphorus doped carbon supported Pd towards formic acid oxidation. Electrochim Acta 213:21–30. https://doi.org/10.1016/j.electacta.2016.06.041
51. Song P, Zhu L, Bo X, Wang A, Wang G, Guo L (2014) Pt nanoparticles incorporated into phosphorus-doped ordered mesoporous carbons: enhanced catalytic activity for methanol electrooxidation. Electrochim Acta 127:307–314. https://doi.org/10.1016/j.electacta.2014.02.068
52. Choi CH, Park SH, Woo SI (2012) Phosphorus-nitrogen dual doped carbon as an effective catalyst for oxygen reduction reaction in acidic media: effects of the amount of P-doping on the physical and electrochemical properties of carbon. J Mater Chem 22(24):12107–12115. https://doi.org/10.1039/c2jm31079a
53. Wu J, Yang Z, Sun Q, Li X, Strasser P, Yang R (2014) Synthesis and electrocatalytic activity of phosphorus-doped carbon xerogel for oxygen reduction. Electrochim Acta 127:53–60. https://doi.org/10.1016/j.electacta.2014.02.016
54. Antoniassi RM, Oliveira Neto A, Linardi M, Spinacé EV (2013) The effect of acetaldehyde and acetic acid on the direct ethanol fuel cell performance using PtSnO2/C electrocatalysts. Int J Hydrog Energy 38(27):12069–12077. https://doi.org/10.1016/j.ijhydene.2013.06.139
55. Jiang Q, Jiang L, Qi J, Wang S, Sun G (2011) Experimental and density functional theory studies on PtPb/C bimetallic electrocatalysts for methanol electrooxidation reaction in alkaline media. Electrochim Acta 56(18):6431–6440. https://doi.org/10.1016/j.electacta.2011.04.135
56. Silva JCM, Ntais S, Teixeira-Neto É, Spinacé EV, Cui X, Neto AO, Baranova EA (2017) Evaluation of carbon supported platinum–ruthenium nanoparticles for ammonia electro-oxidation: combined fuel cell and electrochemical approach. Int J Hydrog Energy 42(1):193–201. https://doi.org/10.1016/j.ijhydene.2016.09.135
57. Assumpção MHMT, da Silva SG, de Souza RFB, Buzzo GS, Spinacé EV, Neto AO, Silva JCM (2014) Direct ammonia fuel cell performance using PtIr/C as anode electrocatalysts. Int J Hydrog Energy 39(10):5148–5152. https://doi.org/10.1016/j.ijhydene.2014.01.053
58. Silva JCM, da Silva SG, De Souza RFB, Buzzo GS, Spinacé EV, Neto AO, Assumpção MHMT (2015) PtAu/C electrocatalysts as anodes for direct ammonia fuel cell. Appl Catal A Gen 490:133–138. https://doi.org/10.1016/j.apcata.2014.11.015
59. Estejab A, Botte GG (2016) DFT calculations of ammonia oxidation reactions on bimetallic clusters of platinum and iridium. Comput Theor Chem 1091:31–40. https://doi.org/10.1016/j.comptc.2016.06.030
60. Lomocso TL, Baranova EA (2011) Electrochemical oxidation of ammonia on carbon-supported bi-metallic PtM (M = Ir, Pd, SnOx) nanoparticles. Electrochim Acta 56(24):8551–8558. https://doi.org/10.1016/j.electacta.2011.07.041
61. Lamb RN, Ngamsom B, Trimm DL, Gong B, Silveston PL, Praserthdam P (2004) Surface characterisation of Pd–Ag/Al2O3 catalysts for acetylene hydrogenation using an improved XPS procedure. Appl Catal A Gen 268(1–2):43–50. https://doi.org/10.1016/j.apcata.2004.03.041
62. Batista J, Pintar A, Mandrino D, Jenko M, Martin V (2001) XPS and TPR examinations of γ-alumina-supported Pd-Cu catalysts. Appl Catal A Gen 206(1):113–124. https://doi.org/10.1016/S0926-860X(00)00589-5
63. Hasik M, Bernasik A, Drelinkiewicz A, Kowalski K, Wenda E, Camra J (2002) XPS studies of nitrogen-containing conjugated polymers—palladium systems. Surf Sci 507–510:916–921. https://doi.org/10.1016/S0039-6028(02)01372-9
64. Al-Hinai MN, Hassanien R, Wright NG, Horsfall AB, Houlton A, Horrocks BR (2013) Networks of DNA-templated palladium nanowires: structural and electrical characterisation and their use as hydrogen gas sensors. Faraday Discuss 164:71–91. https://doi.org/10.1039/c3fd00017f
65. Vankar VD, Vook RW (1983) EELS and AES study of epitaxially grown Pd(111) thin films. Surf Sci 131(2–3):463–474. https://doi.org/10.1016/0039-6028(83)90291-1
66. Zhang L, Li F (2010) Helical nanocoiled and microcoiled carbon fibers as effective catalyst supports for electrooxidation of methanol. Electrochim Acta 55(22):6695–6702. https://doi.org/10.1016/j.electacta.2010.06.002
67. Assumpção MHMT, Moraes A, De Souza RFB, Reis RM, Rocha RS, Gaubeur I, Calegaro ML, Hammer P, Lanza MRV, Santos MC (2013) Degradation of dipyrone via advanced oxidation processes using a cerium nanostructured electrocatalyst material. Appl Catal A Gen 462–463:256–261. https://doi.org/10.1016/j.apcata.2013.04.008
68. dos Reis FVE, Antonin VS, Hammer P, Santos MC, Camargo PHC (2015) Carbon-supported TiO2–Au hybrids as catalysts for the electrogeneration of hydrogen peroxide: investigating the effect of TiO2 shape. J Catal 326:100–106. https://doi.org/10.1016/j.jcat.2015.04.007
69. Antoniassi RM, Otubo L, Vaz JM, Oliveira Neto A, Spinacé EV (2016) Synthesis of Pt nanoparticles with preferential (1 0 0) orientation directly on the carbon support for direct ethanol fuel cell. J Catal 342:67–74. https://doi.org/10.1016/j.jcat.2016.07.022
70. Oliveira Neto A, Brandalise M, Dias RR, Ayoub JMS, Silva AC, Penteado JC, Linardi M, Spinacé EV (2010) The performance of Pt nanoparticles supported on Sb2O5.SnO2, on carbon and on physical mixtures of Sb2O5.SnO2 and carbon for ethanol electro-oxidation. Int J Hydrog Energy 35(17):9177–9181. https://doi.org/10.1016/j.ijhydene.2010.06.028
71. Monyoncho EA, Ntais S, Soares F, Woo TK, Baranova EA (2015) Synergetic effect of palladium–ruthenium nanostructures for ethanol electrooxidation in alkaline media. J Power Sources 287:139–149. https://doi.org/10.1016/j.jpowsour.2015.03.186
72. Modibedi RM, Masombuka T, Mathe MK (2011) Carbon supported Pd–Sn and Pd–Ru–Sn nanocatalysts for ethanol electrooxidation in alkaline medium. Int J Hydrog Energy 36(8):4664–4672. https://doi.org/10.1016/j.ijhydene.2011.01.028
73. Assumpção MHMT, da Silva SG, De Souza RFB, Buzzo GS, Spinacé EV, Santos MC, Neto AO, Silva JCM (2014) Investigation of PdIr/C electrocatalysts as anode on the performance of direct ammonia fuel cell. J Power Sources 268:129–136. https://doi.org/10.1016/j.jpowsour.2014.06.025
74. Zheng L, Xiong L, Liu Q, Han K, Liu W, Li Y, Tao K, Niu L, Yang S, Xia J (2011) Enhanced electrocatalytic activity for the oxidation of liquid fuels on PtSn nanoparticles. Electrochim Acta 56(27):9860–9867
75. Leal da Silva E, Cuña A, Rita Ortega Vega M, Radtke C, Machado G, Tancredi N, de Fraga MC (2016) Influence of the support on PtSn electrocatalysts behavior: ethanol electro-oxidation performance and in-situ ATR-FTIRS studies. Appl Catal B Environ 193:170–179. https://doi.org/10.1016/j.apcatb.2016.04.021